Supporting Information

Vectorially Imprinted Hybrid Nanofilm for Acetylcholinesterase Recognition

K. J. Jetzschmann, G. Jágerszki, D. Dechtrirat, A. Yarman, N. Gajovic-Eichelmann, H.-D.Gilsing, B.Schulz, R.E. Gyurcsányi and F. W. Scheller*

Homology between *Electrophorus electricus* acetylcholinesterase and human AChE

As a model for human acetylcholinesterase (PDB-code: 4PQE), the homotetrameric enzyme from electric eel (*Electrophorus electricu*s, PDB-code: 1C2O) was applied in this study due to the fact that the major portion of the human AChE in the adult brain (reflected in the cerebrospinal fluid) exists in homotetrameric association state, which decreases during AD progression, leading to a shift into dimeric and monomeric species.[1,2] The two enzymes share high sequence similarity of 88.5 % (based on structural alignment performed with ClustalW2 alignment tool, provided by EMBL-EBI) as well as structural similarity (determined using the Secondary Structure Matching tool of PDBeFold service for comparing protein structures in 3D based on best C_α-alignment, provided by EMBL-EBI) with an RMSD value of 0.64 and a Q-score of 0.93 (for C_α-alignment, where 1 is the value for identical structures). Both enzymes possess the so-called peripheral anionic binding site, where propidium as well as the amyloid-β-peptide Aβ42 have been reported to bind.

Protein imprinting via immobilized linkers

Despite of the importance of generating effective synthetic receptors for bio-macromolecules less than 2 % of the MIP literature involves macromolecular imprinting, which reflects the difficulties of imprinting biomolecules.[3] It has been reported that uniform orientation of the

templates during polymer formation results in homogeneous binding sites.[4] For this reason the protein has been bound to a SAM with an "anchor group" (affinity ligand):

Oriented binding of the proteases trypsin and chymotropsin (ChT) respectively via immobilized irreversible inhibitor was used for the preparation of "monoclonal" protein MIPs: ChT was electrostatically bound to the surface of carboxylic acid functionalized MWCTs via the positively charged residues in the active site.[5] The binding capacity of the MIP-covered MWCTs is almost 6 times higher than for the control NIP.

Polymer formation around trypsin which was immobilized to aprotinin-modified glass beads resulted in highly accessible cavities with narrow (monoclonal) distribution of binding affinities and low cross-reactivity.[6]

A different architecture combining AChE with a MIP has been recently presented by Yao et al. AChE was covalently coupled to a SAM on a gold electrode and it was interacted with chlorpyrophos-loaded MIP nanoparticles. Surprisingly the MIP-bound inhibitor effectively suppressed the enzymatic activity maybe by leaching from the MIP.[7]

Xie et al. genetically modified the enzyme methyl-parathion hydrolase by introducing a cystein-terminated linker.[8] It allows the oriented binding of the protein to a silanized glass surface. Photo-polymerization of methacrylic acid derivatives resulted in a MIP with an IF of 1.7.

HRP was covalently bound via its carbohydrate sites to the wall of benzoboroxol-functionalized capillaries or to glass slides and a MIP generated around the enzyme. In alkaline solution the affinity to the immobilized boronate linker and the non-covalent binding to the polymer are synergistic. At pH 7 where only the interaction with the MIP cavities is effective an imprinting factor of 4.6 is obtained.[9]

Recently a "precisely controlled" MIP for glutathione S-transferase was developed using surface-anchored glutathione as the affinity ligand for the enzyme on the gold electrode.

Living radicalic polymerization around the oriented target resulted in a MIP with an imprinting factor of 2-3 and good selectivity against other proteins.[10]

Synthesis of ProDOT-COOH

The **4** was obtained from the ProDOT-dioxyethylene-iodo derivative **1** by O-alkylation of ethyl 4-hydroxybenzoate leading to intermediate **2** (ref. 2), further alkaline saponification to give **3** and finally neutralization of **3** using aqueous sodium hydroxide.[11, 12]

*4-(2-[2-3-Methyl-3,4-dihydro-2H-thieno[3.4-b][1,4]dioxepine-3-ylmethoxy)-ethoxy]-ethoxy)-benzoic acid***3**

A solution of 0.35 g (0.8 mmol) of thiophene ester derivative **2** and 0.13 g (2.3 mmol) of potassium hydroxide in 25 ml of anhydrous EtOH was heated to reflux for 5 hours. After cooling the solution was acidified by adding 0.6 ml (7.2 mmol) of concentrated hydrochloric acid. The solution was evaporated to dryness and the crude product was dissolved in 15 ml of CH_2Cl_2. The solution was filtrated over Celite in order to remove inorganic side products. The filtrate was evaporated to give 0.31 g (=94%) of **3** as a colourless solid.
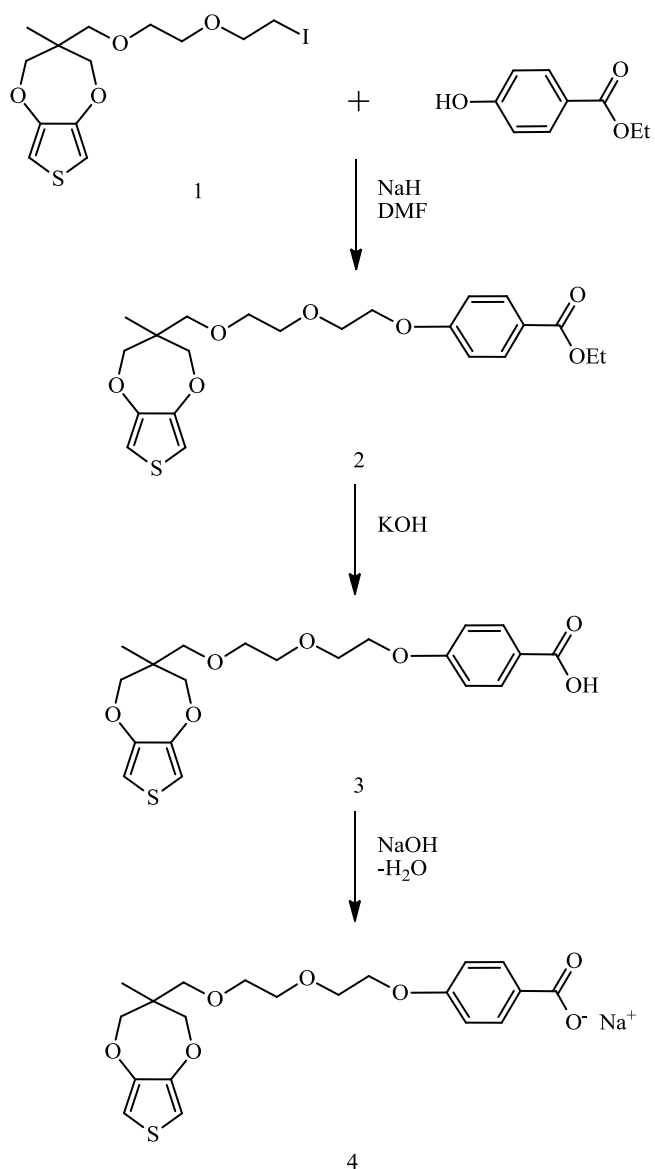
$C_{20}H_{24}O_7S$ (408.47)

mp. 82.5–84.5°C

^{1}H-NMR (DMSO), δ (ppm): 0.89 (3H, s, CCH$_3$), 3.45 (2H, s, CCH$_2$O), 3.55-4.18 (12H, m, OCH$_2$CH$_2$OCH$_2$CH$_2$O, OCH$_2$C (2x)), 6.72 (2H, s, SCH (2x)), 7.01 (2H, d, J = 8.8 Hz, ArH), 7.87 (2H, d, J = 8.8 Hz), ArH), 12.58 (1H, s, br., COOH)

^{13}C-NMR (DMSO), δ (ppm): 16.7, 42.8, 67.4, 68.8, 69.7, 70.5, 72.7, 76.1, 106.0, 114.2, 123.0, 131.3, 149.7, 162.0, 166.9

IR (neat), $\tilde{\nu}$(cm^{-1}): 3106, 2963-2873, 2659, 2514, 1682, 1606, 1484, 1428, 1378, 1321, 1303, 1257, 1171, 1110, 1055, 1029, 920, 846, 771, 651

*4-(2-[2-3-Methyl-3,4-dihydro-2H-thieno[3.4-b][1,4]dioxepine-3-ylmethoxy)-ethoxy]-ethoxy)-benzoic acid sodium salt***4**

A solution of 0.21 g (0.51 mmol) of thiophene carboxylic acid **3** and 0.02 g (0.51 mmol) of sodium hydroxide in 300 ml water was heated to reflux for 1 hour. After cooling the solution was evaporated and the residue was suspended successively in dry acetone and dry ether to give 0.22 g (=100%) of **4** as a colourless solid.

$C_{20}H_{23}O_7NaS$ (430.47)

mp. >300°C

^{1}H-NMR (DMSO), δ (ppm): 0.89 (3H, s, CCH$_3$), 3.46 (2H, s, CCH$_2$O), 3.55-4.09 (12H, m, OCH$_2$CH$_2$OCH$_2$CH$_2$O, OCH$_2$C (2x)), 6.73 (2H, s, SCH (2x)), 6.80 (2H, d, J = 8.8 Hz, ArH), 7.82 (2H, d, J = 8.8 Hz), ArH)

^{13}C-NMR (DMSO), δ (ppm): 19.0, 45.5, 70.0, 71.7, 72.5, 73.3, 76.0, 79.6, 109.6, 116.8, 132.2, 133.9, 151.5, 163.2, 177.4

IR (neat), $\tilde{\nu}$(cm^{-1}): 3107, 2963-2871, 1594, 1547, 1484, 1417, 1252, 1103, 1021, 848, 778, 651

Determination of the thickness of the electropolymerized films by AFM

The thicknesses were measured by removing mechanically a rectangular area of the imaged polymer film using a TAP190AI-G tip (Force Constant is 48 N/m, 225 μm long) in contact mode and then rescanning the same surface in tapping mode. The removal of the film was accomplished by using a force of 2 μN in five consecutive cycles and it is made possible by the fact that the polymer film is less stiff than both the tip and the gold substrate. The 2 μN was the largest force that could be applied without having the gold substrate also removed. As shown in Figure S2, even after 20 cycles the same depth profile is registered for the MIP film which indicates that the removal is constricted to the polymer film. The higher thicknesses at the edge of the step are due to the accumulation of material during scratching.
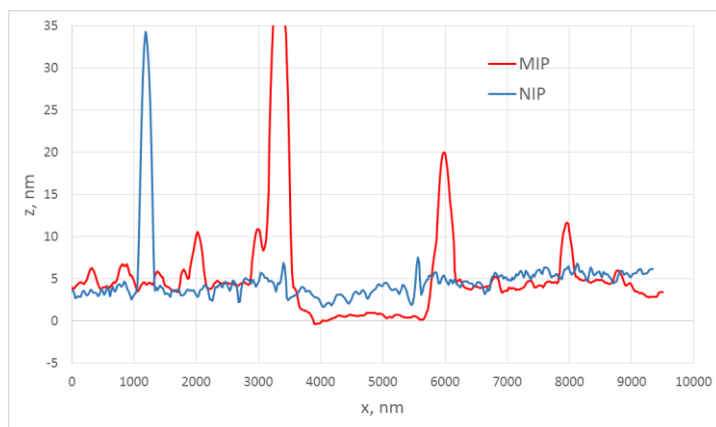
Figure S1. Depth profiles of the rectangular area after several removal cycles performed at 2 µN applied force.

Figure S2 shows the topographic images after removal of the polymer films from MIP and NIP surfaces under the optimized nanolithography conditions. Analysis of the line profiles of the recorded AFM images is shown in Figure S3.
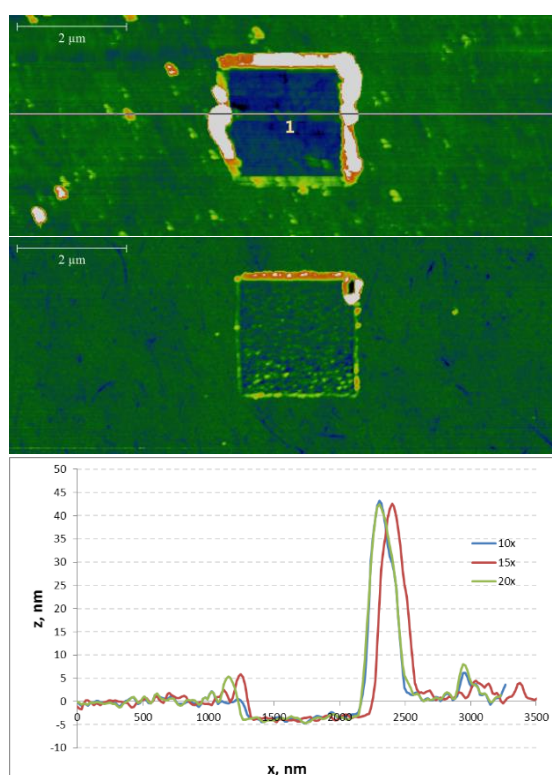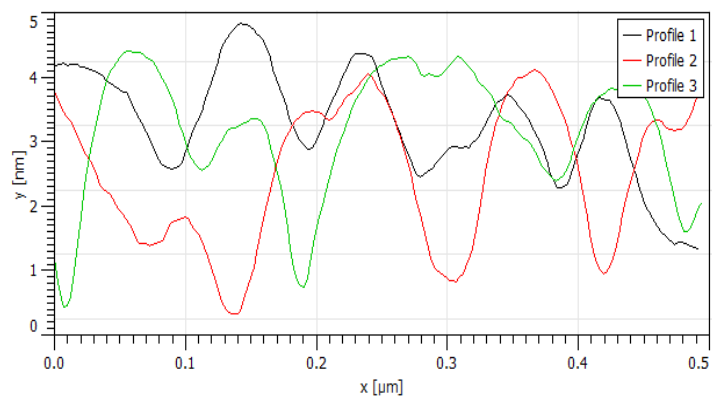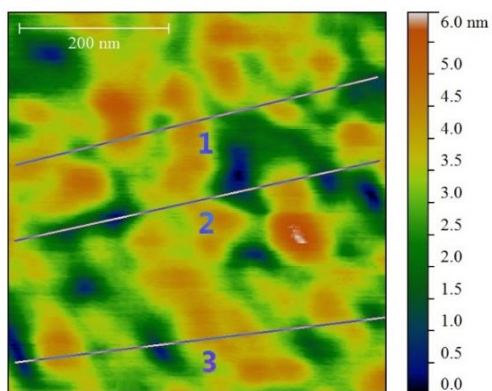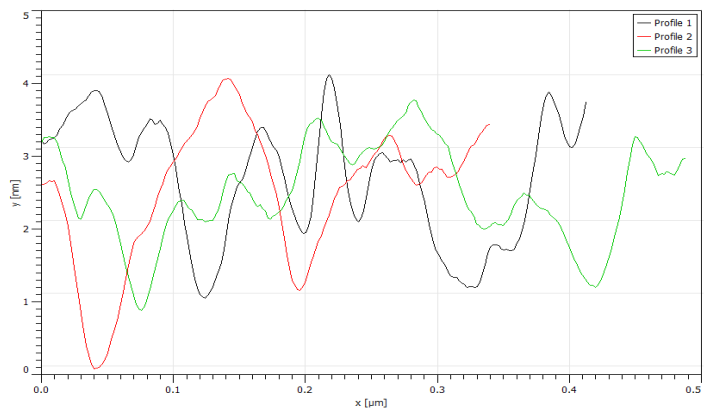

Figure S2. Topography of the MIP (top) and NIP (middle) films after removal of the polymeric film in a rectangular area by nanolithography and depth profiles along the indicated lines (bottom).
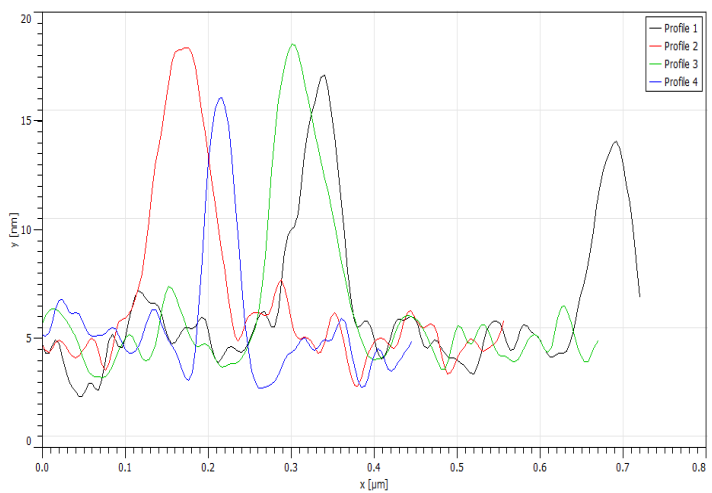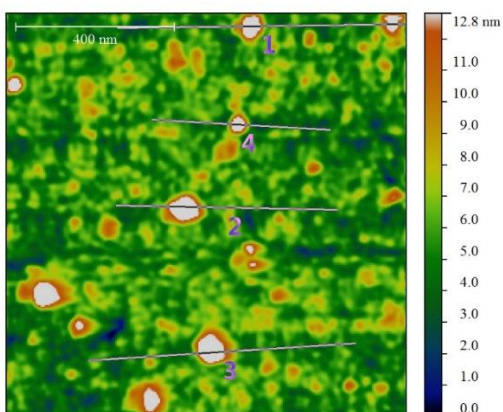
NIP

MIP
(AChE
removed)

MIP +
AChE
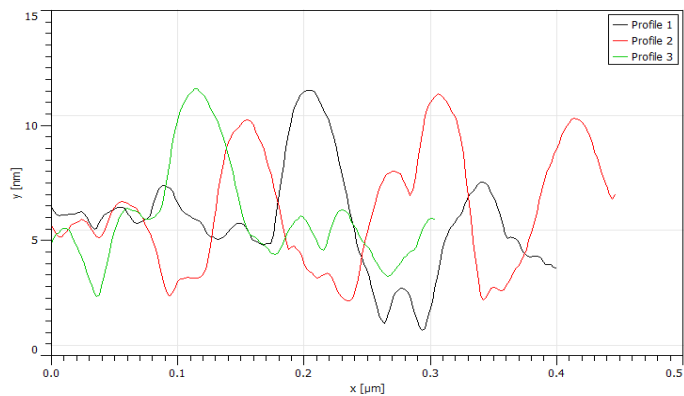Electrode
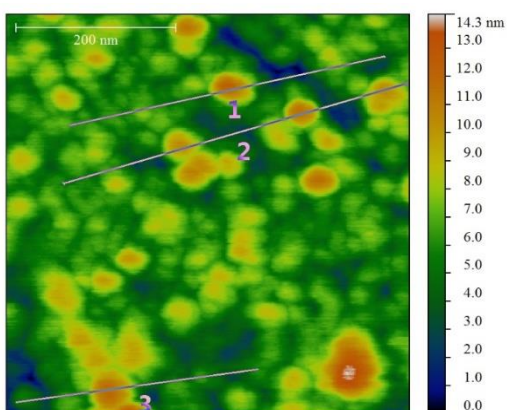#1

MIP +
AChE
Electrode
#2

Figure S3. Representative topographies and line profiles of MIP films with removed and rebound AChE. In case of MIPs with removed template the profiles reveal cavities that are not present when the AChE is rebound, but instead they show features (peaks) with heights that indicate the presence of bound AChE molecules. The lateral resolution is not sufficient to further substantiate the profiles.

Curve fitting of the amperometric response of MIP and NIP covered electrodes

Curve fitting was performed using OriginPro 8 software. The corresponding fitting parameters for the non-linear fit ($y = B_{max} * x / (k + x)$, model OneSiteBind) were B_{max} = 171.33 ± 53.27 µg/mL and k = 0.42 ±0.18 $µM^{-1}$ with R^2 = 0.94792 for MIP and B_{max} = 8.67 ± 1.67 µg/mL and k = 0.0086 ± 0.0072 $µM^{-1}$ with R^2 = 0.0552 for NIP, respectively.

[1] E.B. Fishman, G.C. Siek, R.D. MacCallum, E.D. Bird, L. Volicer, J.K. Marquis, *Ann. Neurol.* **1986**, *19*, 264-252.

[2] J. Sáez-Valero, G. Sberna, C. A. McLean, D.H. Small, *J. Neurochem.* **1999**, *2*, 1600-1608.

[3] D. R. Kryscio, N. A. Peppas, *Acta Biomater.* **2012**, *8*, 461.

[4] M. J. Whitcombe, I. Chianella, L. Larcombe, S. A. Piletsky, J. Noble, R. Porter, A. Horgan, *Chem. Soc. Rev.* **2011**, *40*, 1547.

[5] C. Zheng, X. L. Zhang, W. Liu, B. Liu, H. H. Yang, Z. A. Lin, G. N. Chen. *Adv. Mat*. **2013**, *25*, 5922.

[6] A. Guerreiro, A. Poma, K. Karim, E. Moczko, J. Takarada, I. Perez de Vargas-Sansalvador, N. Turner, E. Piletska, C. Schmidt de Magalhães, N. Glazova, A. Serkova, A. Omelianova, S. Piletsky, *Adv. Healthc. Mater*, **2014**, *3*, 1426.

[7] G. H. Yao, R. P. Liang, C. F. Huang, Y. Wang, J. D. Qiu. *Anal.Chem*. **2013**, *85*, 11944.

[8] L. Liu, J. Zheng, G. Fang, W. Xie, *Anal. Chim. Acta*. **2012**, *726*, 85.

[9] S. Wang, J. Ye, Z. Biea, Z. Liu, *Chem. Sci.***2014,** *5*, 1135.

[10] Y. Kamon, R. Matsuura, Y. Kitayama, T. Ooya, T. Takeuchi, *Polym. Chem.***2014**, *5*, 4764.

[11]   F. G. Guler, H.-D. Gilsing, B. Schulz, A. S. Sarac, *J. Nanosci. Nanotechnol.* **2012**, *12*, 7869.

[12]   M.-D. Damaceanu, H.-D. Gilsing, B. Schulz, A. Arvinte, M. Bruma, *RSC Adv.* **2014**, *4*, 52467.